Electronic Supplementary Material (ESI) for Journal of Materials Chemistry C.

Strain-induced tunable valley polarization and topological phase transition in $SVSiN_2$ monolayer

Yunxi Qi, Can Yao and Jun Zhao*

Jiangsu Provincial Engineering Research Center of Low Dimensional Physics and New Energy & School of Science, Nanjing University of Posts and Telecommunications, Nanjing, Jiangsu 210023, China

Hui Zeng†

School of Microelectronics, Nanjing University of Science and Technology, Nanjing, Jiangsu 210094, China‡

Authors to whom correspondence should be addressed: zhaojun@njupt.edu.cn (Jun Zhao) and zenghui@njust.edu.cn (Hui Zeng)

Table S1 The lattice constant of the $SVSiN_2$ monolayer, V-N bond length $R_{V\text{-}N}$, V-S bond length $R_{V\text{-}S}$, layer thickness h, and PBE bandgap without SOC.

$SVSiN_2$	$a=b$ (Å)	$R_{V\text{-}N}$ (Å)	$R_{V\text{-}S}$ (Å)	h (Å)	E_g (eV)
without dipole correction	2.952	2.02	2.34	4.95	0.53
With dipole correction	2.952	2.02	2.33	4.94	0.52

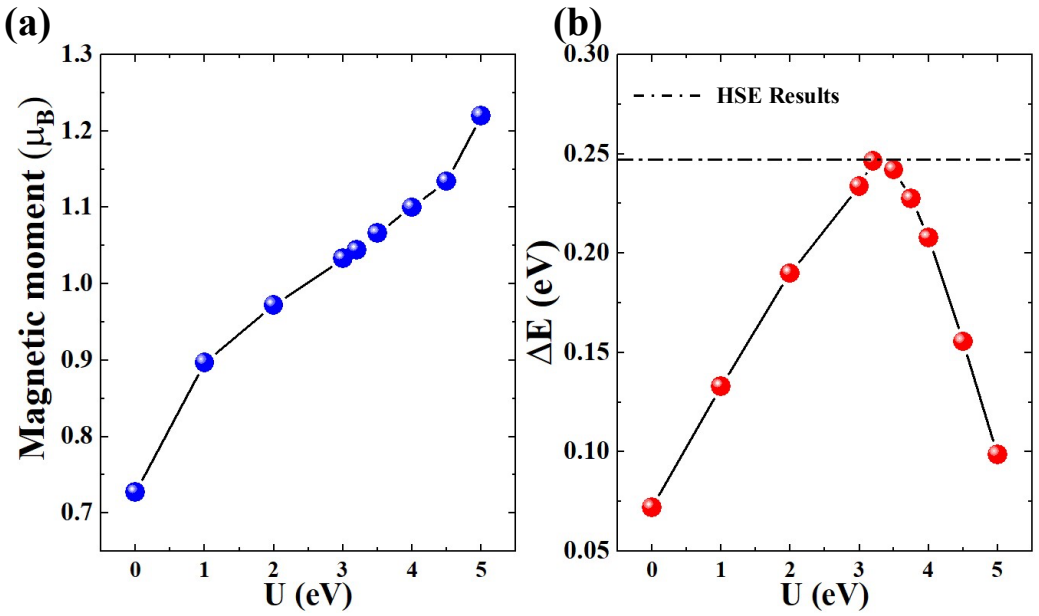

Fig S1. The (a) local magnetic moment of the V ions, and (b) the energy difference between AFM and FM configurations of the $SVSiN_2$ monolayer with respect to the different U_{eff} values.

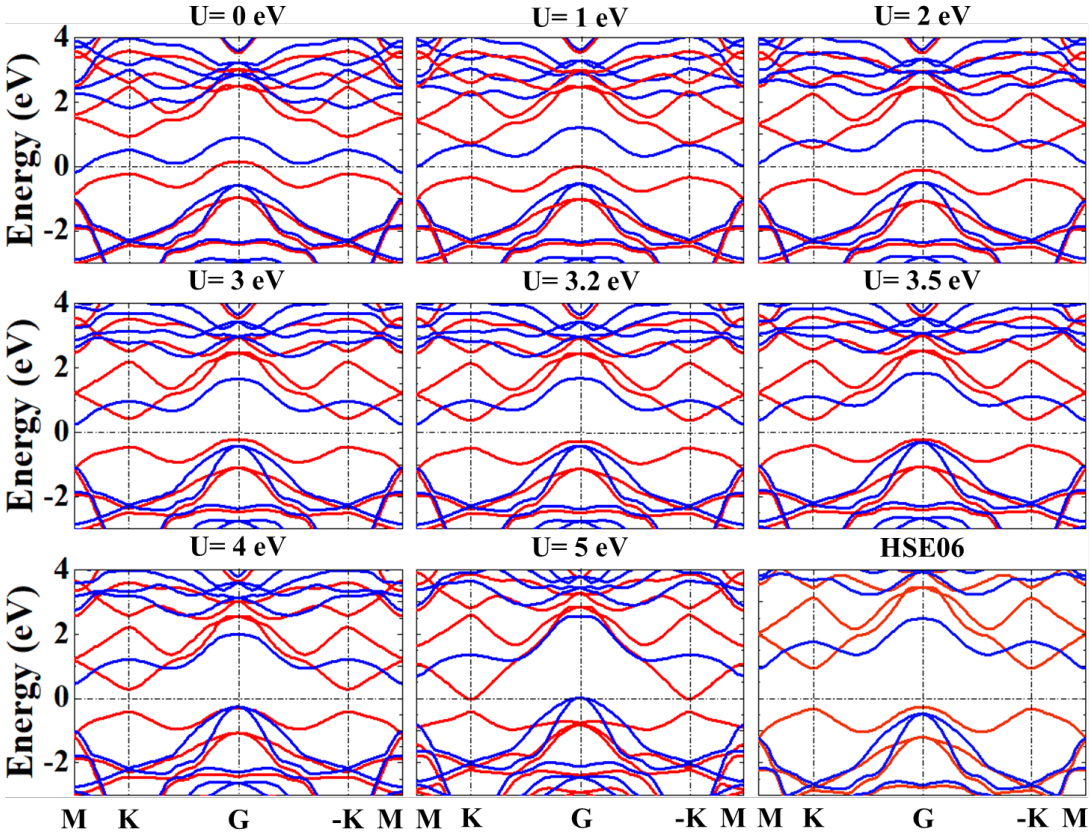

Fig S2. Band structures of the $SVSiN_2$ monolayer by using different U_{eff} values and by using HSE06 hybrid functional.

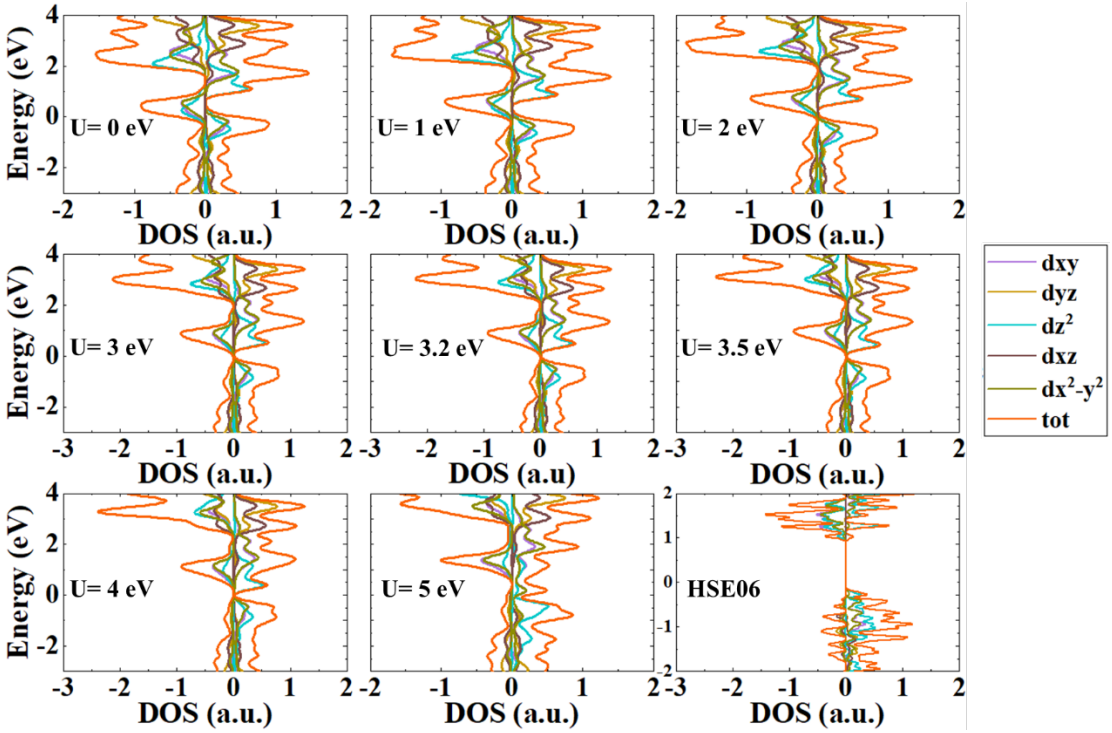

Fig S3. Projected density of state of the $SVSiN_2$ monolayer by using different U_{eff} values and by using HSE06 hybrid functional.

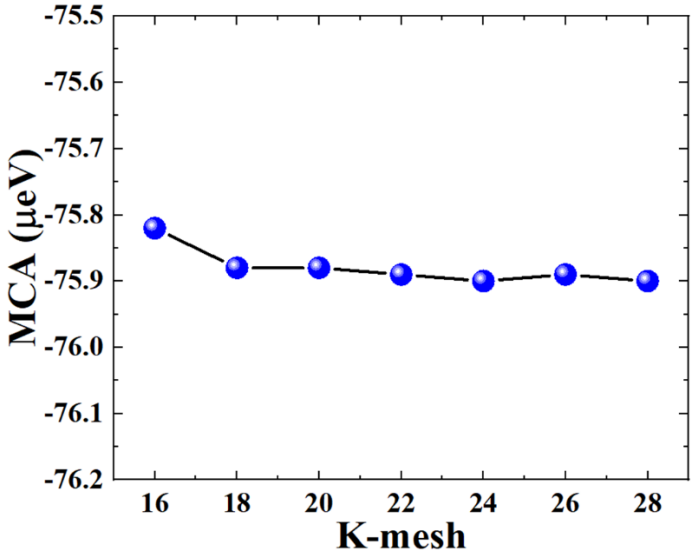

Fig S4. Magnetic crystal anisotropy (MCA) performance of the $SVSiN_2$ monolayer under different *k*-grids.

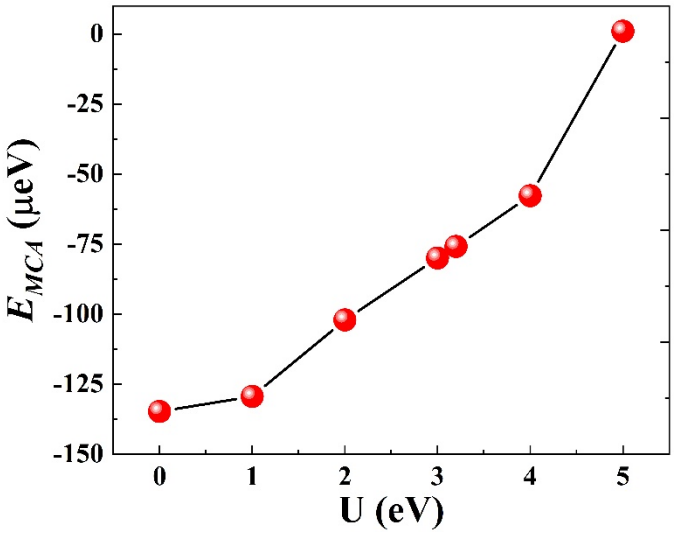

Fig. S5 The E_{MCA} of the $SVSiN_2$ monolayer as a function of different U_{eff} values.

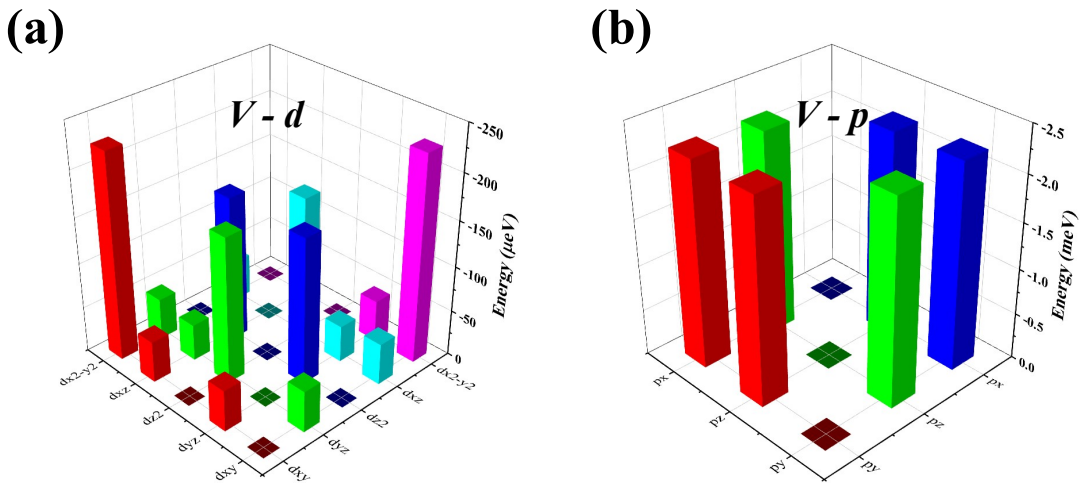

Fig S6. The orbital-resolved spin orbit coupling (SOC) energy difference of V atoms in the $SVSiN_2$ monolayer, where (a) is the V-*d* orbital, and (b) is the V-*p* orbital. All orbitals are beneficial for in-plane MCA.

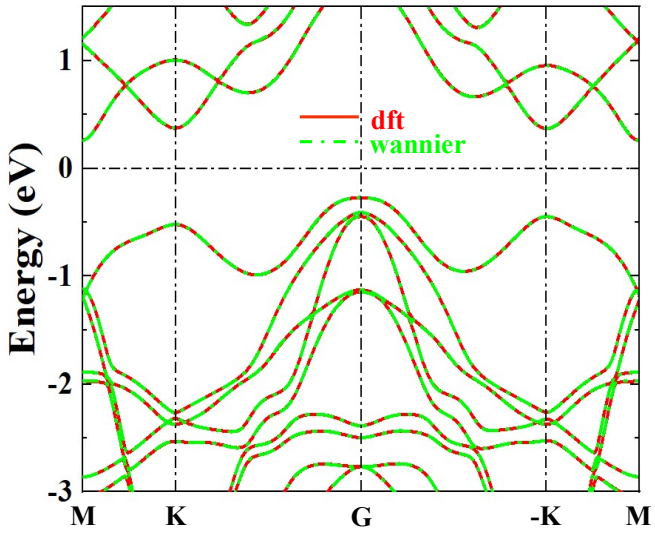

Fig S7. The band structure of the $SVSiN_2$ monolayer calculated by first principles (solid red line) and tight-binding method implemented by WANNIER90 (green dotted line).

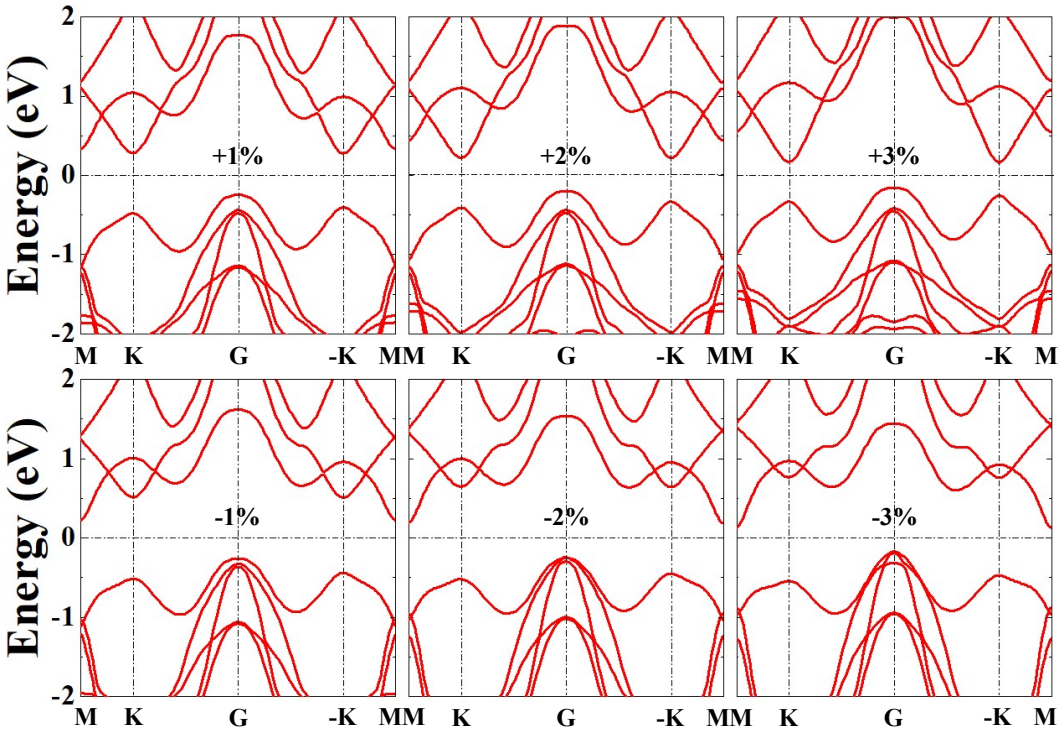

Fig S8. The band structures of the $SVSiN_2$ monolayer under different in-plane biaxial strains.

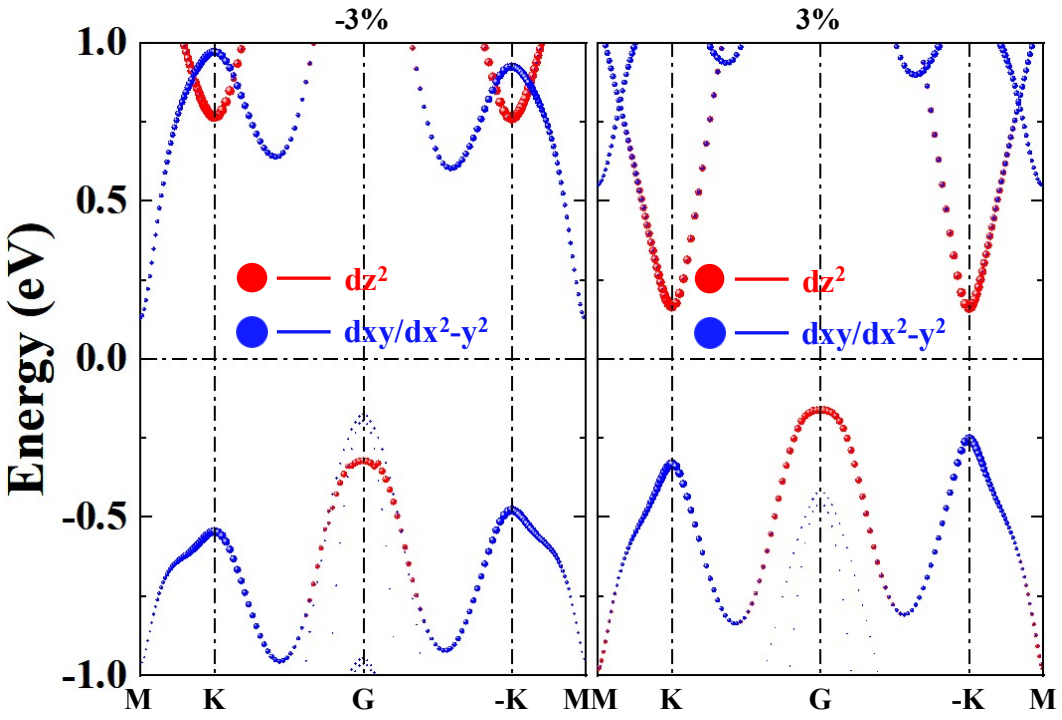

Fig S9. The projected band structures of the $SVSiN_2$ monolayer under -3% and 3% biaxial strain.

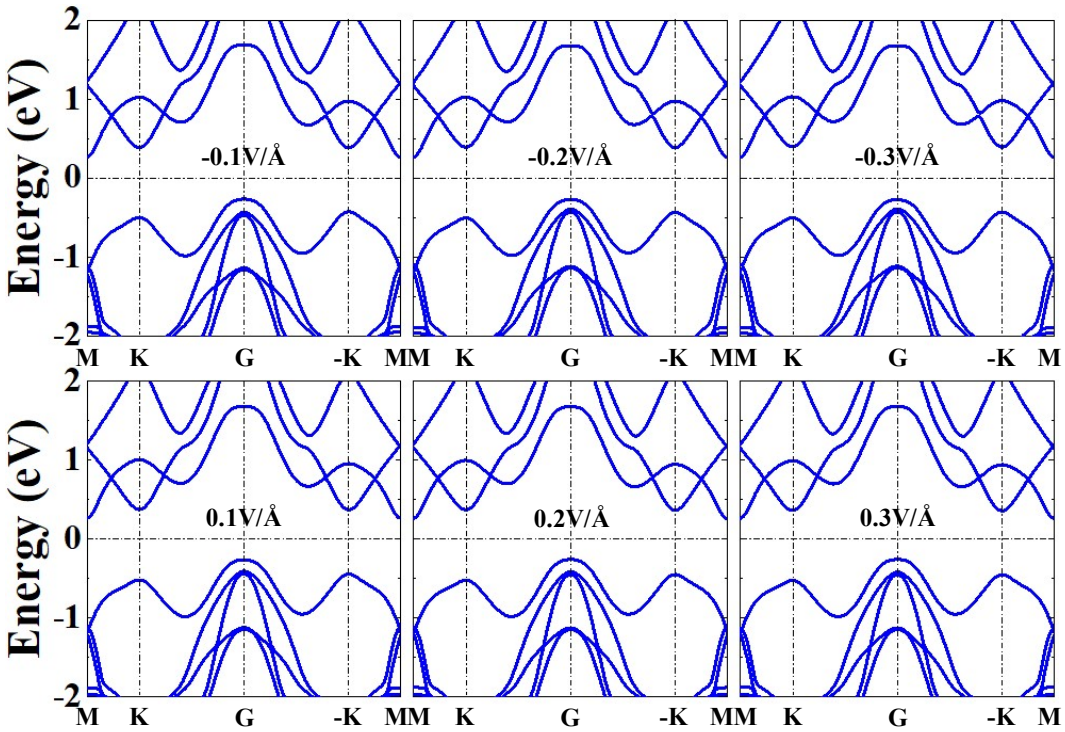

Fig S10. The band structures of the $SVSiN_2$ monolayer under different vertical electric fields.